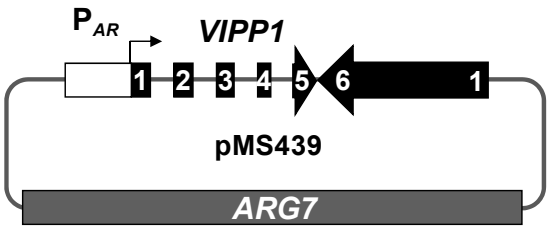

Supplemental Figure 1. Construct used for the suppression of *VIPP1* by RNAi. A piece of *VIPP1* genomic DNA in sense orientation was fused to a *VIPP1* cDNA fragment in antisense orientation. Exons are drawn as black boxes, introns and non-coding sequences as grey lines. Constitutive expression was driven by a fusion of promoters *HSP70A* and *RBCS2* (*AR*) shown as white box. The *ARG7* gene (grey box) was located on the same plasmid as selectable marker. Introns in the *ARG7* gene are not shown.

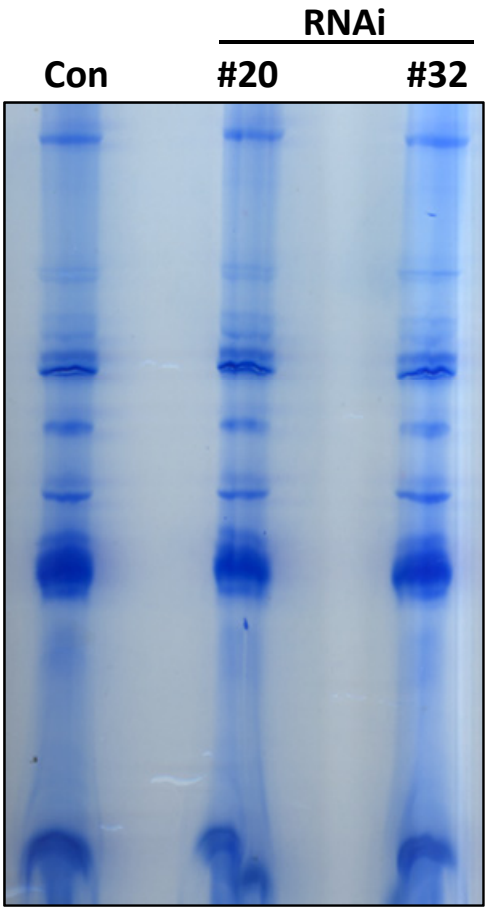

Supplemental Figure 2. Major thylakoid membrane protein complexes are fully assembled in *VIPP1*-RNAi strains. A control strain and *VIPP1*-RNAi strains #20 and #32 grown in TAP-NH_4 medium were separated into soluble and membrane fractions by freeze-thawing cycles. Proteins in membrane fractions were solubilized in β-dodecyl-maltoside, separated on a 3-14% blue-native polyacrylamide gradient gel and stained with Colloidal Coomassie blue.

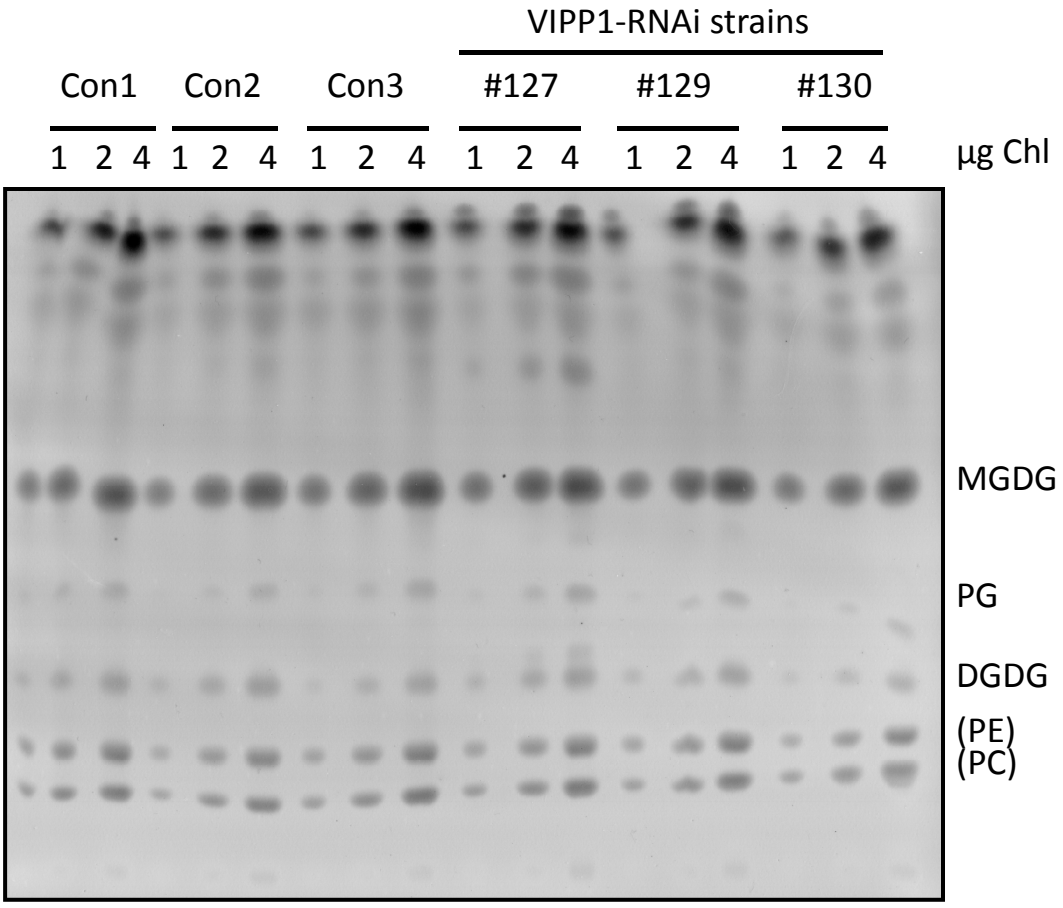

Supplemental Figure 3. Bulk membrane lipid composition in *VIPP1*-RNAi strains is indistinguishable from that of control strains. Whole cell lipids from three biological replicates of a control strain and from *VIPP1*-RNAi strains #127, #129, and #130 were extracted, separated by thin layer chromatography and visualized with iodine vapor. Monogalactosyl-diacylglycerol (MGDG), phosphatidylglycerol (PG) and digalactosyl-diacylglycerol (DGDG) were identified based on their comigration with the respective purchased lipids. Phosphatidylcholin (PC) and phosphatidylethanolamine (PE) were assigned according to migrations reported by Gaude et al. (2004).

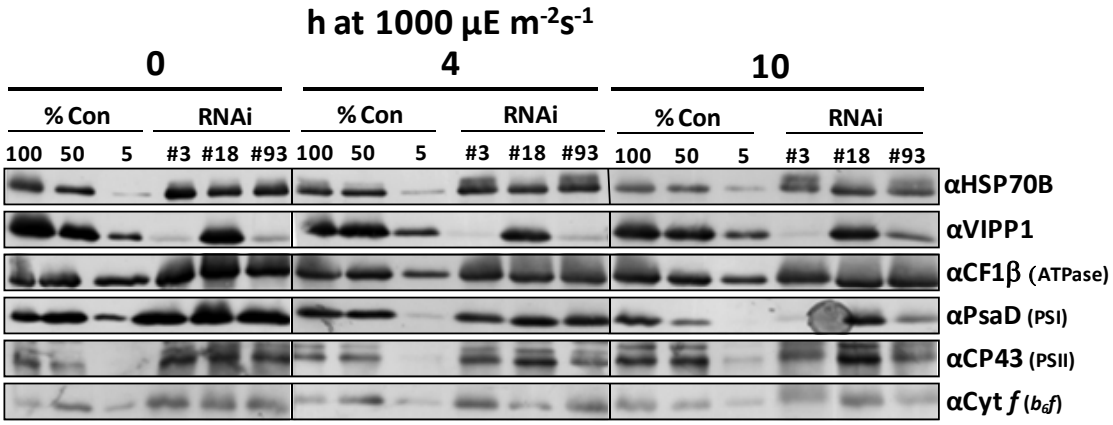

Supplemental Figure 4. Subunits of PSII and PSI are rapidly degraded in *VIPP1*-RNAi strains exposed to high light intensities. A control strain and *VIPP1*-RNAi strains #3, #18, and #93 were grown in TAP-NH_4 medium and exposed to a light intensity of ~1000 µE m^{-2} s^{-1} for 10 h. 53.5 µg whole-cell proteins from each sample were separated on a 7.5-15% SDS-polyacrylamide gel and analyzed by immunoblotting.

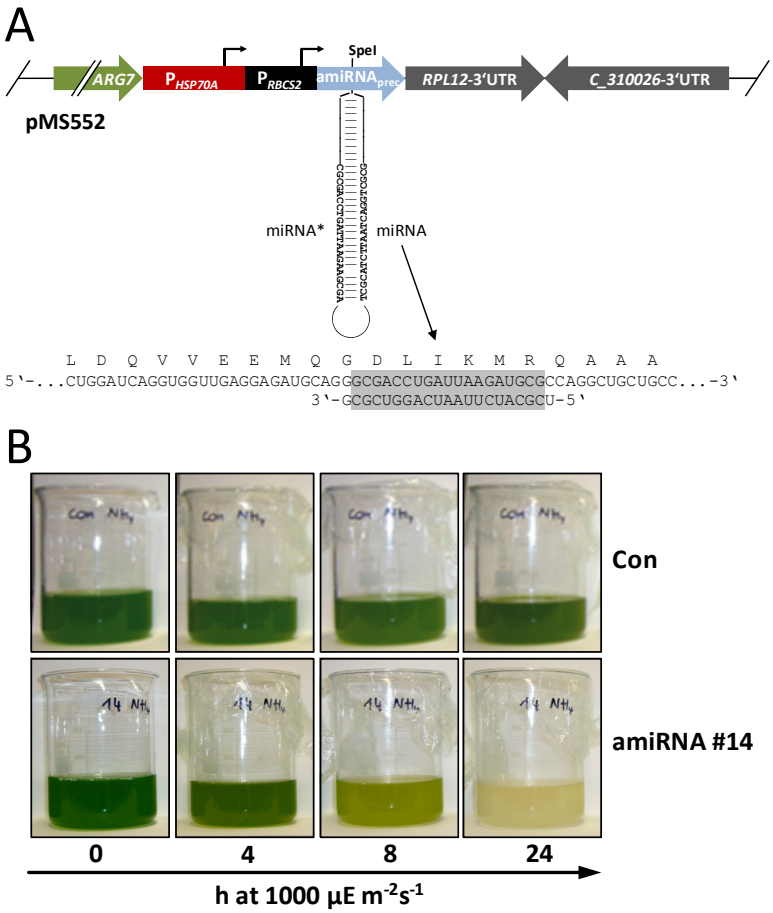

Supplemental Figure 5. High-light sensitivity is also observed in *VIPP1*-amiRNA strains unable to induce VIPP2 expression.

(A) Schematic drawing of the amiRNA construct used and its target region in the *VIPP1* transcript. pMS552 is based on pChlamiRNA2 (Molnar et al., 2009), which is driven by the constitutively active *HSP70A-RBCS2* tandem promoter. The amiRNA generated by pMS552 targets the VIPP1 coding region. Base-pairing nucleotides of the amiRNA and *VIPP1* mRNA are shaded in grey.

(B) High-light sensitivity of *VIPP1*-amiRNA strains. A control strain and *VIPP1*-amiRNA strain #14 grown in TAP-NH_4 medium were exposed to a light intensity of ~1000 µE m^{-2} s^{-1} for 24 h.

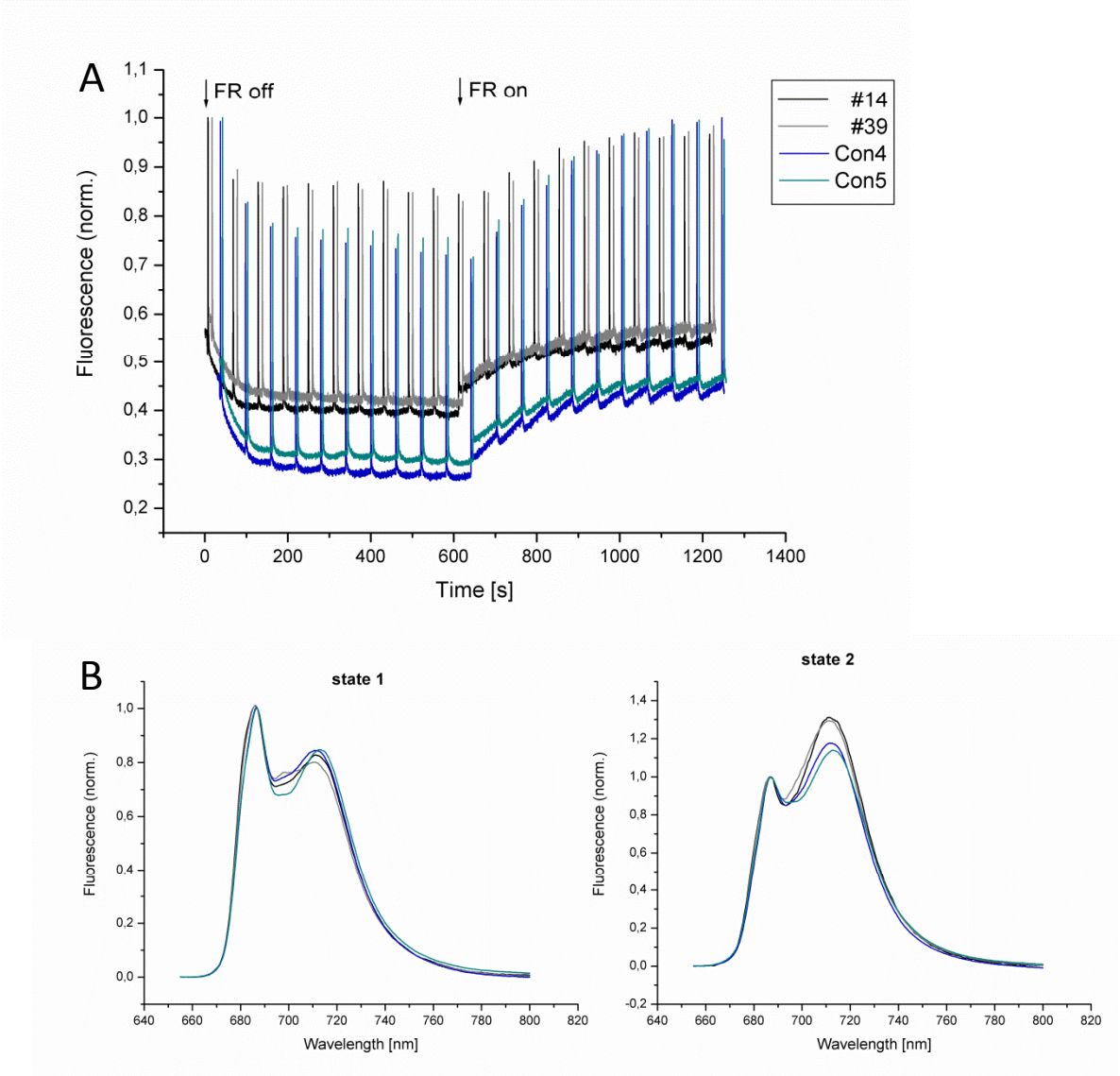

Supplemental Figure 6. *VIPP1*-RNAi strains are not impaired in state transitions.
(A) PAM fluorescence traces. Control and *VIPP1*-RNAi strains #14 and #39 were grown in TAP-NH_4 medium at ~30 µE m^{-2} s^{-1}. After 10 min exposure to far red light (FR) to establish state 1, FR was switched off to establish state 2. After 10 min, FR was switched on again. The PAM traces were normalized to the initial F_M.
(B) 77 K fluorescence emission spectra. Samples were taken from cultures illuminated with far red light for 10 min in the presence of 10 µM DCMU (state 1), or bubbled with nitrogen for 10 min in the dark (state 2) and immediately frozen in liquid nitrogen. Spectra were recorded with excitation at 430 nm and normalized at 687 nm.

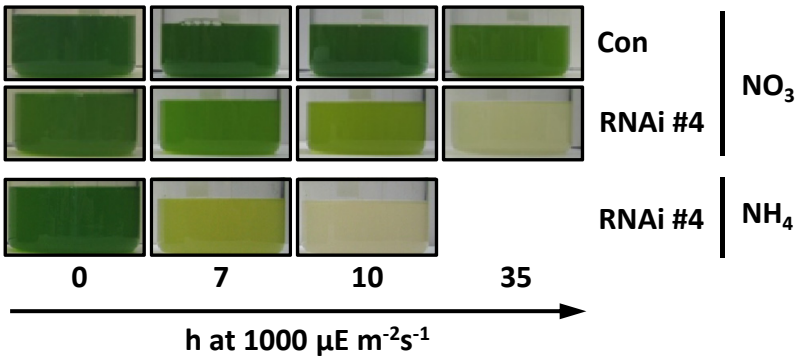

Supplemental Figure 7. Delayed bleaching of *VIPP1*-RNAi strains grown on nitrate. A control strain and *VIPP1*-RNAi strain #4 were grown in TAP-NO_3 medium and exposed to a light intensity of ~1000 µE m^{-2} s^{-1} for 35 h. Pictures of high-light exposed strain #4 grown in TAP-NH_4 from Figure 1C are shown for comparison.

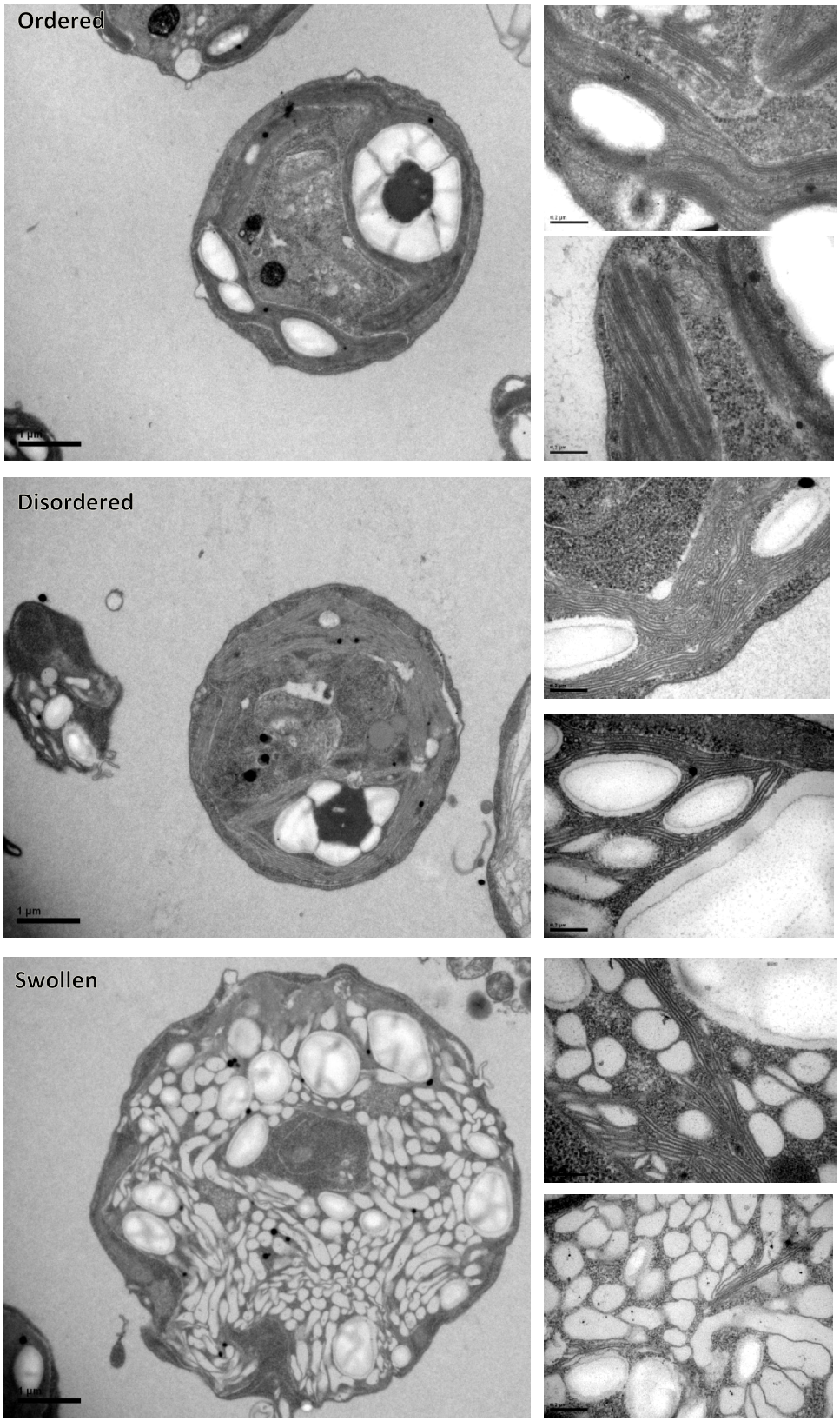

Supplemental Figure 8. Categories of thylakoid structure.
Shown are electron microscopy images from cells of control and *VIPP1*-RNAi/amiRNA strains that represent typical examples for the three categories of 'ordered', 'disordered' and 'swollen' thylakoids. Scale bars in overview images correspond to 1 µm, those in zoom-ins to 0.2 µm.

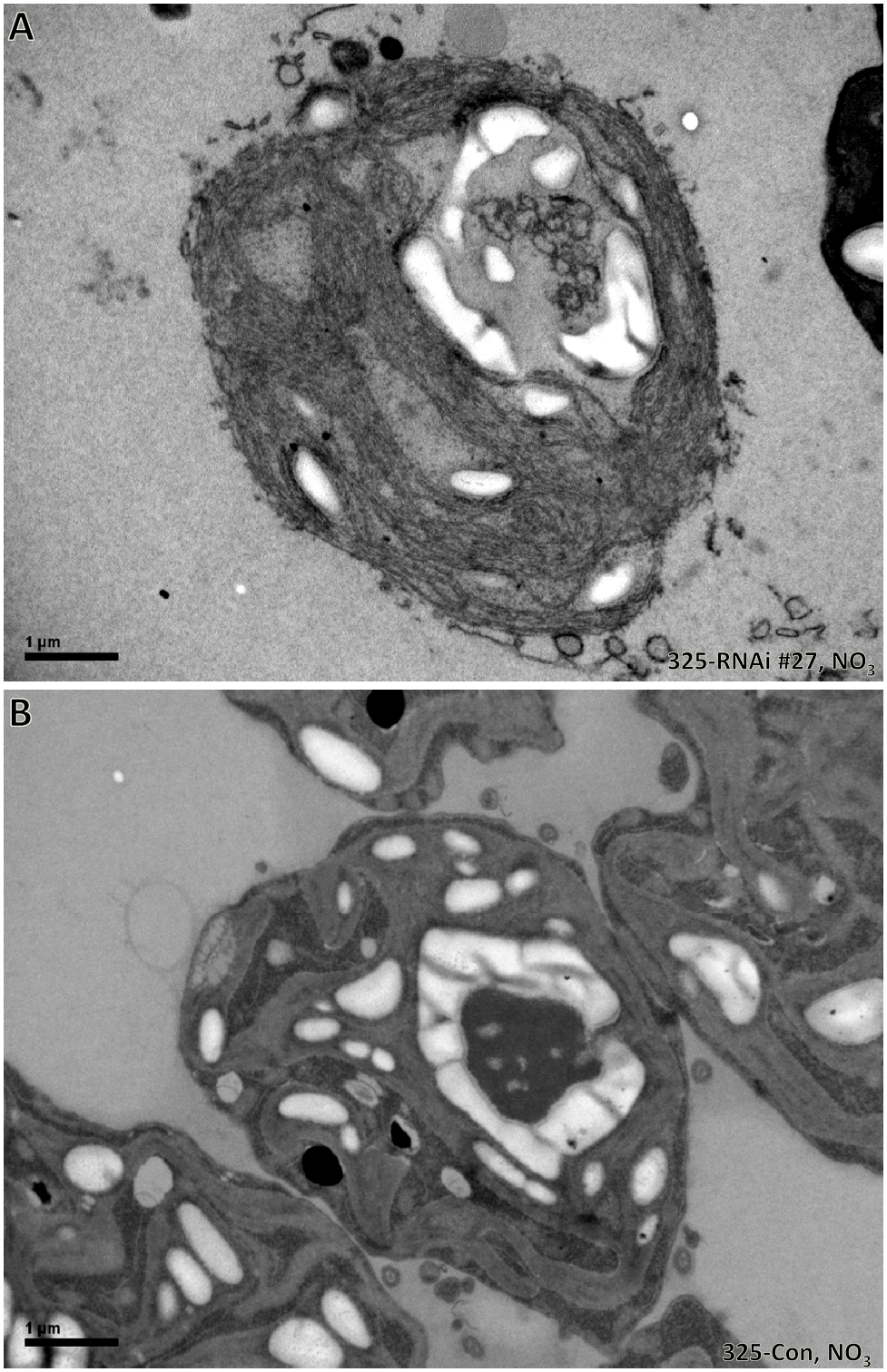

Supplemental Figure 9. Lysis of high light-exposed *VIPP1*-RNAi cells grown on nitrate appears not to be caused by thylakoid swelling.

(A) Electron microscopy image of a cell from *VIPP1*-RNAi strain #27. Cells were grown in TAP-NO_3 medium and exposed to ~1000 µE m^{-2} s^{-1} for 7 h. Shown is a typical image of a lysed cell. Lysis was observed for 36 out of 100 randomly photographed cells.

(B) Electron microscopy image of a cell from the control strain. Cells were treated as in (A). Shown is a typical image of an intact cell. 98-99 of 100 randomly photographed control cells were intact.

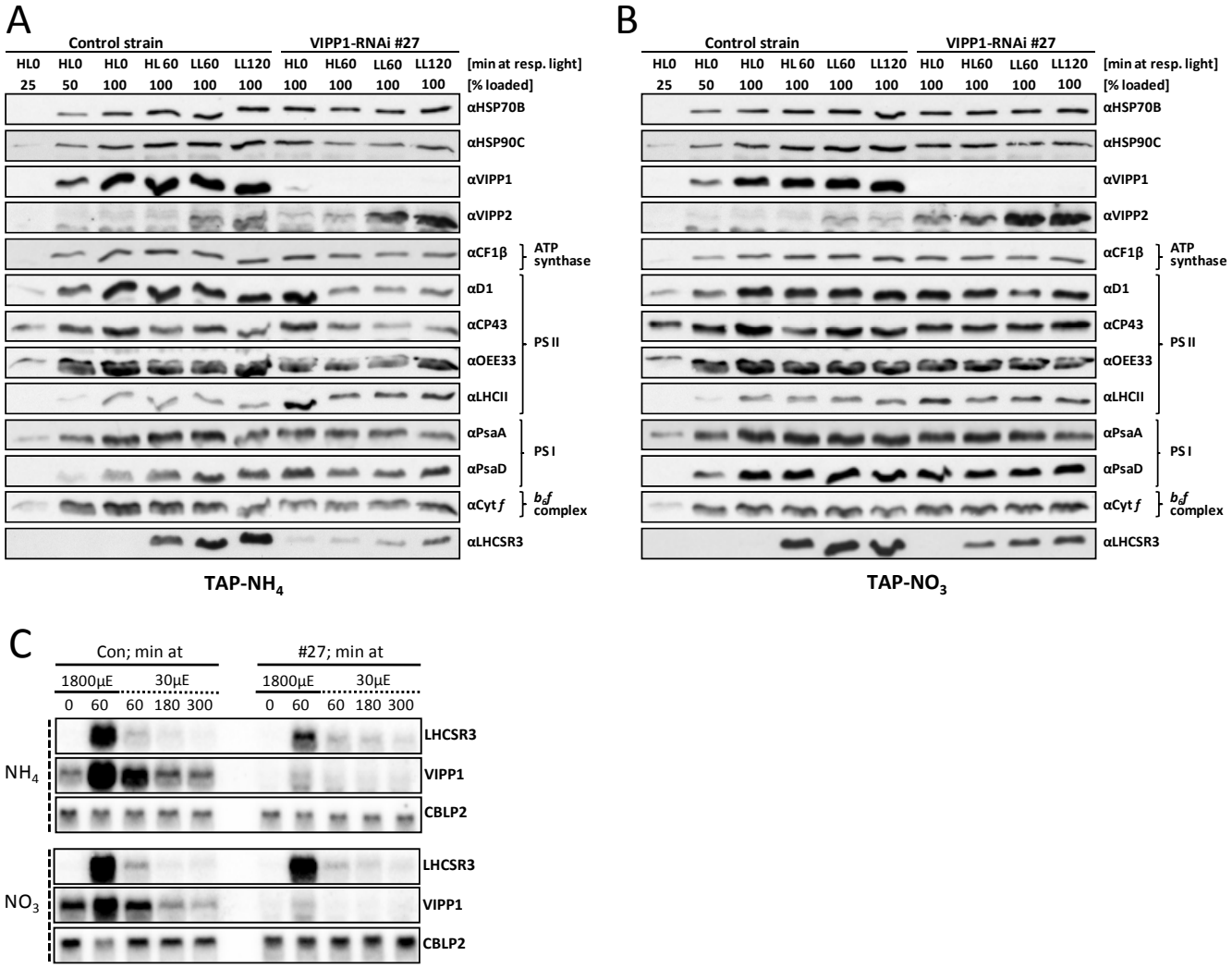

Supplemental Figure 10. *VIPP1*-RNAi strains are less sensitive to photoinhibition when grown on nitrate as compared to ammonium.

(A) Subunits mainly of PSII but also of PSI are degraded in *VIPP1*-RNAi strains after photoinhibition. Control and *VIPP1*-RNAi strain #27 were grown in TAP-NH_4 medium. Cells were exposed to ~1800 µE m^{-2} s^{-1} for 60 min (HL) and shifted back to ~30 µE m^{-2} s^{-1} for 120 min (LL). Whole-cell proteins were separated on 14% SDS-polyacrylamide gels and analyzed by immunoblotting.

(B) Subunits of PSII and PSI are less prone to degradation in photoinhibited *VIPP1*-RNAi strains grown on nitrate. The experiment was done as described in (A), but cells were grown in TAP-NO_3 medium.

(C) RNA gel blot analysis of photoinhibited control and *VIPP1*-RNAi strains. Control and *VIPP1*-RNAi strain #27 were grown in TAP-NO_3 or TAP-NH_4 medium. Cells were exposed to ~1800 µE m^{-2} s^{-1} for 60 min and shifted back to ~30 µE m^{-2} s^{-1} for 300 min for recovery. RNA was extracted from samples taken at the indicated time points and subjected to RNA gel blot analysis. *CBLP2* served as loading control.

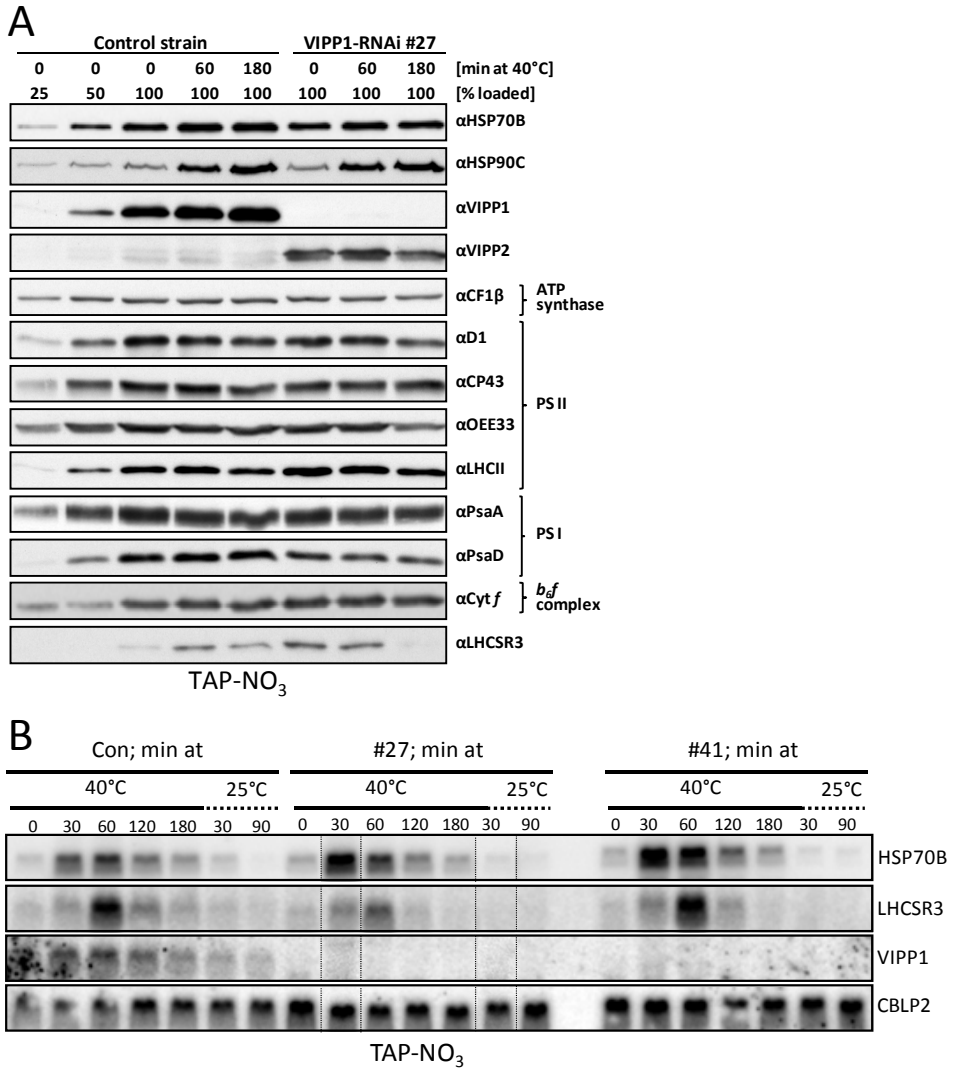

Supplemental Figure 11. *VIPP1*-RNAi strains are less sensitive to heat shock when grown on nitrate as compared to ammonium.

(A) Subunits of thylakoid membrane complexes are not affected by heat stress in *VIPP1*-RNAi strains grown on nitrate. Control and *VIPP1*-RNAi strain #27 were grown in TAP-NO_3 medium. Cells were exposed to 40°C and whole-cell proteins were extracted at the indicated time points. Whole-cell proteins were separated on 14% SDS-polyacrylamide gels and analyzed by immunoblotting.

(B) RNA gel blot analysis of heat-stressed control and *VIPP1*-RNAi strains. Control and *VIPP1*-RNAi strains #27 and #41 were grown in TAP-NO_3 medium. Cells were exposed to heat shock at 40°C for 180 min and shifted back to 25°C for 90 min. RNA was extracted from samples taken at the indicated time points and subjected to RNA gel blot analysis. *CBLP2* served as loading control.

SUPPLEMENTAL METHODS

Lipid extraction, separation and visualization

VIPP1-RNAi strains #127, #129, and #130 and three biological replicates of a control strain were grown at ~30 µE m^{-2} s^{-1} in TAP-NH_4 medium to a density of ~3 x 10^6 cells/ml. 14 ml of each culture were harvested by centrifugation at 3500 *g*, washed with phosphate buffered saline and the pellet was frozen in liquid N_2 and stored at -80°C. Pellets were resuspended in 600 µl methanol/chloroform/formic acid (1:1:0.1) and 200 µl 0.1 M KCl, 0.2 M H_3PO_4 were added. Samples were homogenized by vortexing, phases were separated by centrifugation and the organic phase was transferred to a glass vial. The remaining aqueous phase was extracted again with 400 µl chloroform/methanol (2:1), organic phases were combined and dried in a constant stream of nitrogen. Lipids were resuspended in chloroform/methanol (2:1) to a concentration of 1 µg/µl chlorophyll. Separation of lipids was done according to (Benning and Somerville, 1992) on $(NH_4)_2SO_4$ treated TLC silica plates (Baker Si250PA) using acetone/toluene/water (91:30:8) as mobile phase. Lipids were visualized with iodine vapor. The standard for phosphatidylglycerol was purchased from Sigma, those for mono- and digalactosyldiacylglycerol were a kind gift from Dr. Sandra Witt, MPI-MP, Potsdam-Golm. Phosphatidylcholin (PC) and phosphatidylethanolamine (PE) were assigned according to migrations reported previously (Gaude et al., 2004).

BN-PAGE

Blue-native PAGE was done according to published protocols (Schagger and von Jagow, 1991; Schagger et al., 1994).

77 K fluorescence and PAM measurements

77 K fluorescence emission spectra were measured using a F-6500 spectrofluorometer (Jasco). The sample was excited at 430 nm wavelength with a 10 nm bandwidth, and emission spectra were measured between 655 and 800 nm wavelength. To monitor state transitions by PAM, measurements were done in a home-made suspension cell with a FMS2 pulse amplitude modulation fluorometer (Hansatech, Norfolk, UK) at 25° C, with alternating far-red light application as described previously (Lokstein et al., 1994). Saturating light pulses were given every 60 sec.

REFERENCES

Benning, C., and Somerville, C.R. (1992). Isolation and genetic complementation of a sulfolipid-deficient mutant of *Rhodobacter sphaeroides*. J Bacteriol **174,** 2352-2360.

Gaude, N., Tippmann, H., Flemetakis, E., Katinakis, P., Udvardi, M., and Dormann, P. (2004). The galactolipid digalactosyldiacylglycerol accumulates in the peribacteroid membrane of nitrogen-fixing nodules of soybean and Lotus. J Biol Chem **279,** 34624-34630.

Lokstein, H., Härtel, H., Hoffmann, P., Woitke, P., and Renger, G. (1994). The role of light-harvesting complex II in excess excitation dissipation: an in-vivo fluorescence study on the origin of high-energy quenching. J Photochem Photobiol B: Biol **26,** 175-184.

Schagger, H., and von Jagow, G. (1991). Blue native electrophoresis for isolation of membrane protein complexes in enzymatically active form. Anal Biochem **199,** 223-231.

Schagger, H., Cramer, W.A., and von Jagow, G. (1994). Analysis of molecular masses and oligomeric states of protein complexes by blue native electrophoresis and isolation of membrane protein complexes by two-dimensional native electrophoresis. Anal Biochem **217,** 220-230.